SUPPLEMENTARY INFORMATION

Combining computational and experimental studies to gain mechanistic insights for n-butane isomerisation with a model microporous catalyst

Matthew E. Potter,[1,2,3]* Lucas Spiske,[4] Philipp N. Plessow,[4] Evangeline B. McShane,[3] Marina Carravetta,[3] Alice E. Oakley,[3] Takudzwa Bere,[5] James H. Carter,[5] Bart D. Vandegehuchte,[6] Kamila M. Kaźmierczak,[6] Felix Studt[4,7]* and Robert Raja[3]

1) Chemistry Department, University College London, Gordon Street, London, WC1H 0AJ, UK

2) UK Catalysis Hub, Research Complex at Harwell, Rutherford Appleton Laboratory, Didcot, OX11 0FA, UK

3) School of Chemistry, University of Southampton, Highfield Campus, Southampton, Hampshire, SO17 1BJ, UK

4) Institute of Catalysis Research and Technology, Karlsruhe Institute of Technology, Hermann-von-Helmholtz-Platz 1, 76344 Eggenstein-Leopoldshafen, Germany

5) Max Planck-Cardiff Centre on the Fundamentals of Heterogeneous Catalysis FUNCAT, Cardiff Catalysis Institute, School of Chemistry, Cardiff University, Main Building, Park Place, Cardiff, CF10 3AT, UK

6) TotalEnergies OneTech Belgium, Zone Industrielle Feluy C, B-7181 Seneffe, Belgium

7) Institute for Chemical Technology and Polymer Chemistry, Karlsruhe Institute of Technology, Engesserstrasse 18, 76131 Karlsruhe, Germany

* MEP = mep61@bath.ac.uk, FS = felix.studt@kit.edu

Contents

MgAlPO-5 Schematic

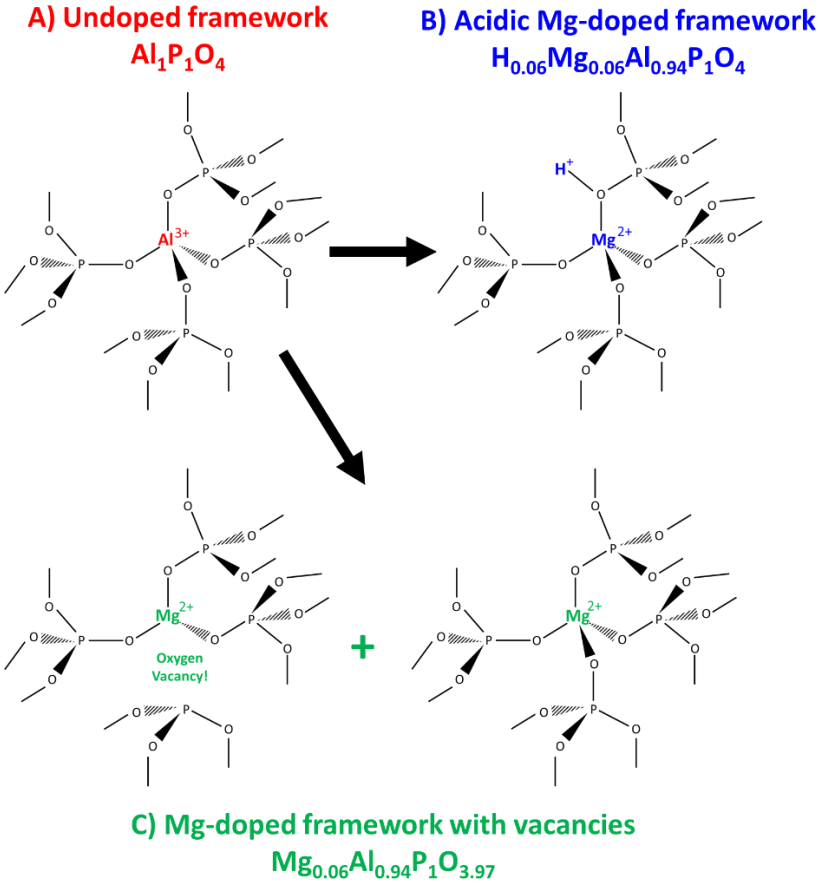

Figure S1. Showing the different substitution pathways possible, on substituting Mg^{2+} into the undoped AlPO framework, showing A) the bare framework (AlPO-5), B) type I substitution of Mg^{2+} for Al^{3+} leading to the formation of a Brønsted acid site (BAS) and C) two sites where Mg^{2+} has undergone type I substitution for Al^{3+}, showing the formation of an oxygen vacancy, forming a Lewis acid site (LAS). Here two sites are shown to balance the charges as $2Al^{3+} + 2O^{2-} \rightarrow 2Mg^{2+} + 1O^{2-}$.

Experimental Methods

Characterisation

Powder X-ray Diffraction (pXRD): pXRD was performed on a Bruker D2 Phaser diffractometer using a 1D LYNXEYE detector and 0.6 mm slits, with Cu Kα1 radiation. Patterns were run over a 2θ range of 5 – 50 ° with a scan speed of 3 °/min and an increment of 0.01 °.

Nitrogen physisorption (BET): Physisorption measurements were performed at 77 K, on a sample dried under 20 mTorr of vacuum at 120 °C overnight. The P/P_0 range spanned from 0.0001 to 0.95. Analysis was performed on a Micromeritics Gemini 2375 surface area analyser. Surface area was calculated using the BET model, while the pore width distribution was calculated with the BJH model.

Scanning Electron Microscopy (SEM): Images were acquired on an SEM FEI Quanta 250 in SEM mode. Stubs were used and coated with an adhesive carbon tab to mount the dry powder samples. The samples were sputter coated with 7 nm Platinum to reduce surface charging when imaging.

Inductively Coupled Plasma-Mass Spectrometry (ICP-MS) analysis: ICP-MS was performed by 10 mg of samples being digested in 1 mL of concentrated HNO_3, 1 mL of concentrated HCl and 0.75 mL of concentrated HF. The samples were heated overnight at 120 ^oC to ensure that complete digestion occurred. Samples were then diluted into 60 mL of deionised water and then diluted 1:100 into 3% HNO_3 in deionised water. These samples were then run on a High Resolution ICP-MS Thermo ELEMENT 2XR, with appropriate standards for quantification. ICP analysis was performed at the National Oceanography Centre, Southampton with the kind help of Dr. Matthew Cooper.

Solid State NMR (ssNMR): ssNMR samples were packed into 4 mm rotors, and acquired at a spinning rate of 8 kHz. ^{27}Al, and ^{31}P spectra were acquired in triple resonance mode on a Bruker Avance Neo Spectrometer, using a 9.4 T field, in air. The sample ^{27}Al and ^{31}P relaxation time was assessed using a saturation recovery pulse technique, which was used for the respective direct acquisitions. ^{27}Al spectra were acquired after 128 scans and ^{31}P spectra were collected with 4 scans, 240 secs between scans.

Pyridine-probed Diffuse Reflectance Infrared Fourier Transform Spectroscopy (DRIFTS) measurements: DRIFTS measurements were recorded in the wavenumber range of 4000 to 1000 cm^{-1} in the Kubelka-Munk format accumulating 64 scans per minute at a spectral resolution of 4 cm^{-1} on a Bruker Tensor 27 spectrometer fitted with a mercury cadmium telluride (MCT) detector cooled by liquid nitrogen. A sample was loaded into the Praying Mantis high-temperature (HVC-DRP-4) in situ cell and evacuated under vacuum (pressure lower than 10^{-6} mbar) at 400 °C for 1 h. The system was then cooled to 150 °C and a background spectrum was recorded under N_2 flow (30 mL min^{-1}). The sample was then exposed to pyridine (8 mL) by the isothermal saturator (14.0 °C) under N_2 flow (30 mL min^{-1}) at 150 °C for 30 min. Excess adsorbate was removed by outgassing at 150 °C for 1 h prior to recording spectra.

Ammonia Temperature Programmed Desorption (NH_3-TPD) acidity measurements: All TPD measurements were performed using an AutoChem II 2920 TPD/TPR instrument (Micromeritics). Calcined materials were pretreated by heating at 10°C/min to 600°C in helium gas for 2 h. The samples were exposed to a 10% NH_3 /helium mixture and allowed to equilibrate at 150°C for 8 h. Desorption was performed in flowing helium by heating with a 4-stages temperature ramp, first at 10°C/min to 250°C, then hold at 250°C for 1h, then at 10°C/min to 600°C and finally held for 40 minutes at 600°C. The well-separated peaks allowed an easy fitting of the raw data.

Catalytic analysis

In our kinetic study we followed a similar procedure to Wulfers *et al.*, purposefully keeping the conversion below 5 mol%. Firstly, this is so there is negligible change in n-butane partial pressure, simplifying the kinetic analysis. Secondly this will suppress any reverse, or secondary reactions,

allowing us to focus purely on the n-butane conversion step. Using this method, we can analyse the data using standard kinetic equations:

$$\frac{d([iC_4])}{dt} = k[nC_4]^z$$

where [iC_4] is the concentration of a product, in this case isobutane, d()/dt refers to the change in concentration with time, k is the reaction constant, [nC_4] is the concentration of the n-butane reactant and z is the reaction order. This becomes:

$$ln\left\{\frac{d([iC_4])}{dt}\right\} = \ln\{k\} + z.\, ln\{[nC_4]\}$$

Therefore, plotting the natural log of the rate of product formation versus the natural log of n-butane concentration yields the reaction order as the gradient of a linear expression.

Conversion of n-Butane, product selectivity and product yield (here referring to unspecified product i) were calculated as:

$$Conversion\ of\ nC_4\ (mol\%) = 100\% \times \frac{Total\ Area - nC_4\ Area}{Total\ Area}$$

$$Product\ Yield\ of\ product\ i\ (mol\%) = 100\% \times \frac{Product\ i\ Area \times R_i}{Total\ Area}$$

where R_i is the response factor of the molecule, in this case R_i corresponds to the carbon number, divided by 4, to normalise it to the initial moles of n-Butane. The intensity of GC FIDs is known to be proportional to carbon number for alkane and alkenes, as such this allows us to convert from area to mol%.

Mass balances, based on the quantity of carbon, were calculated in all cases, by comparing peak areas for an unreacted butane stream, with the sum of peak areas in the reaction samples. This was consistently found to be within 90-110 %, suggesting insignificant amounts of reactant were lost.

For kinetic analysis, the product yield was converted into reaction rates, by multiplying the product yields by butane flow rate in µmol/sec/g.

Computational details

An AFI unit cell containing 48 T-sites has been chosen for this work. Unit cell optimization was performed using the unsubstituted H-SSZ-24 AFI structure $AlO_{96}Si_{48}$ within the VASP program package.[1-5] The symmetry of the unit cell was set by fixing the angles of the cell to α=β=90°; γ=120°. After unit cell optimization, the lengths of the unit cells were a=13.886 Å, b=13.886 Å and c=17.221 Å; the volume was V=2874.219 $Å^3$. From this structure, the H-Mg-AlPO-5 structure was then created by substituting all Si atoms by phosphorus and alumina, so that every phosphorus atom is next to four alumina atoms and vice versa. The acid site aluminum was changed to magnesia. This way, we have a periodic unit cell consisting of 96 O sites and 48 T sites, one half being phosphorus and the other half being alumina, one of which is substituted by Mg; as the AFI structure has only one distinguishable T-site, the choice of the specific aluminum atom is arbitrary. This leads to a ratio of Al/P/Mg 23:24:1. The charge equilibrium is reestablished by an acid proton on an oxygen adjacent to the Mg atom. The

resulting H-MgAlPO-5 structure $HAl_{23}MgO_{96}P_{24}$, after geometry optimisations has lattice parameters of a=b=13.863 Å, c=16.832 Å, V=2801.361 $Å^3$. As there are four different O-sites, calculations have been performed to ensure that we choose the O-site that has the lowest energy. In Table S1, we show the four different crystallographic positions for the proton, together with the energy difference in reference to the lowest energy structure, in which the hydrogen is bound to the O1 atom.

Table S1: Relative energies, given in kJ/mol, for the four different O-sites of MgAlPO-5, with the crystallographic O_1-site taken as the 0 energy reference.

Crystal. O-site	**O1**	**O2**	**O3**	**O4**
ΔE [kJ/mol]	0.0	21.5	3.6	29.6

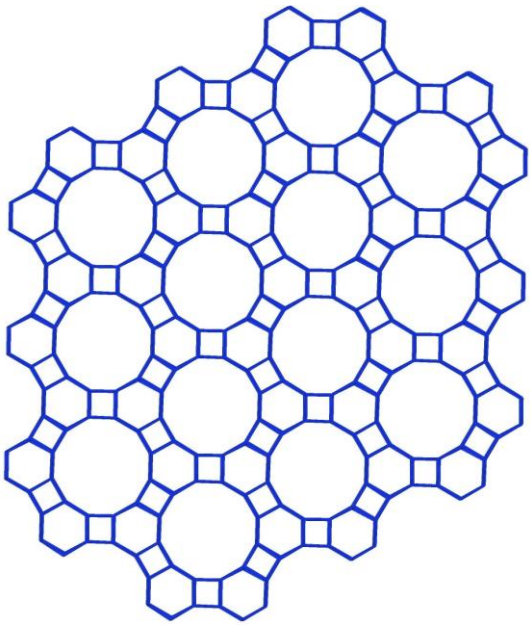

Figure S2: Periodic structure of the AFI zeolite, as seen along the z-axis, showcasing the main channel structure of the zeolite.

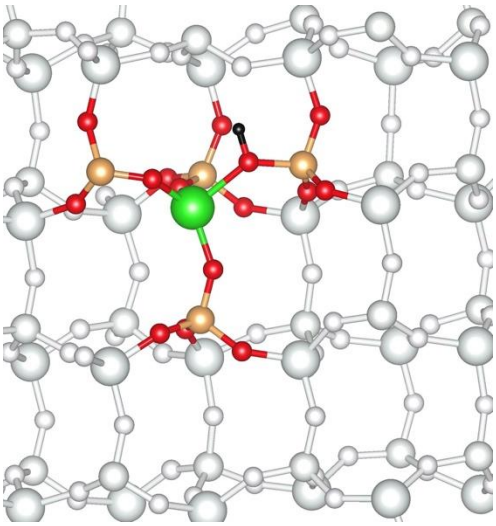

Figure S3: Acid site of the H-MgAlPO-5 zeolite, showcasing the acid proton. Coloring: green – Mg, red – O, orange – P, black – acid H. All other atoms of the periodic zeolite structure are shown in white.

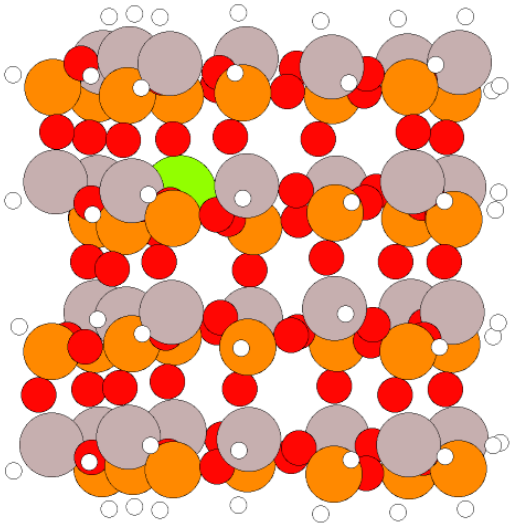

Figure S4: Cluster model of H-Mg-AlPO-5, seen along the X-axis. The number of "layers" along the z-axis has been chosen to be large enough to describe the chemical environment accurately, but small enough to keep the computational cost for the calculations low. Coloring: Mg – green, Al – gray, P – orange, O – red, H – white.

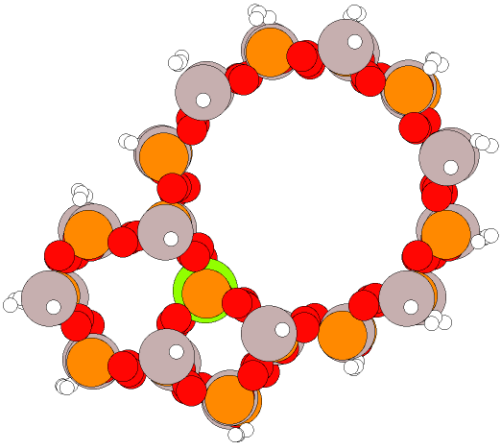

Figure S5: Cluster model of H-Mg-AlPO-5, seen along Z-axis. Coloring: Mg – green, Al – gray, P – orange, O – red, H – white.

Catalyst Integrity

Table S2: Summary of nitrogen physisorption and ICP-MS metal loading for MgAlPO-5 samples.

Sample	BET Surface Area (m^2/g)	Total Pore Volume (cm^3/g)	Micropore Volume (cm^3/g)	Mg (wt%)	Al (wt%)	P (wt%)

1% MgAlPO-5	308	0.25	0.19	0.14	19.5	16.7
3% MgAlPO-5	288	0.22	0.17	0.46	18.7	16.4
6% MgAlPO-5	285	0.21	0.17	0.95	18.1	16.2

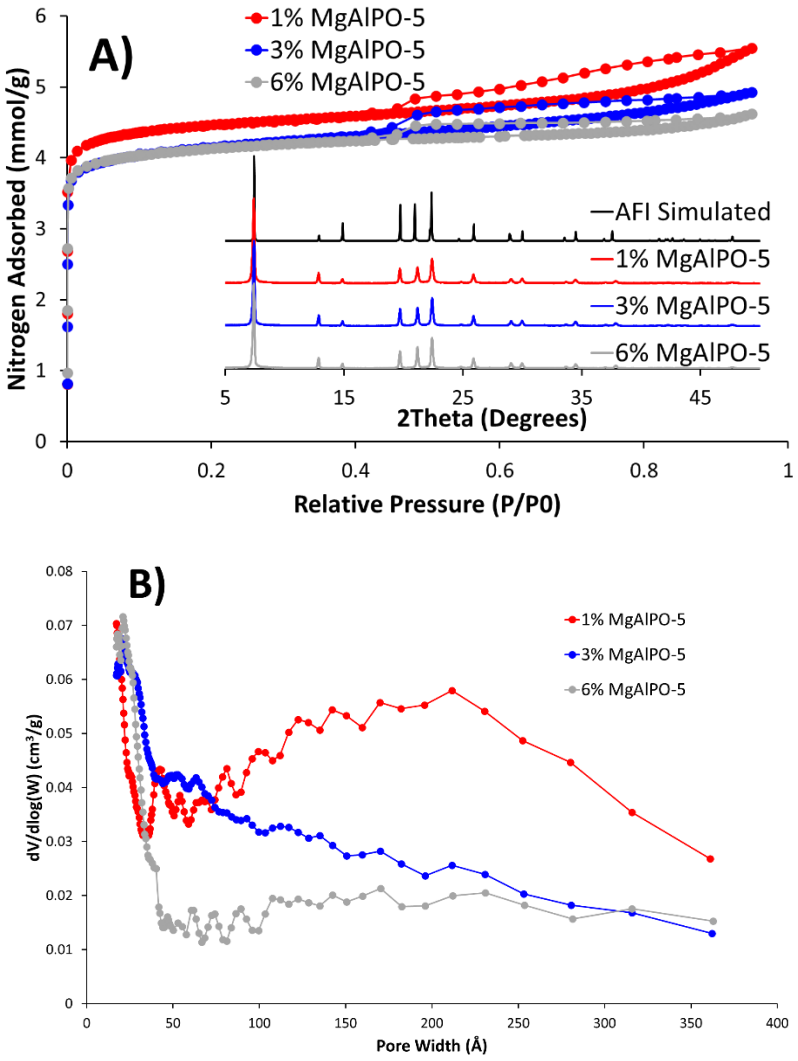

Figure S6: A) Nitrogen physisorption isotherms of 1, 3 and 6% MgAlPO-5 showing microporosity with inset showing powder XRD confirming AFI phase purity of the three samples. B) BJH pore-width distribution plot showing no significant higher-level porosity, beyond the expected microporosity.

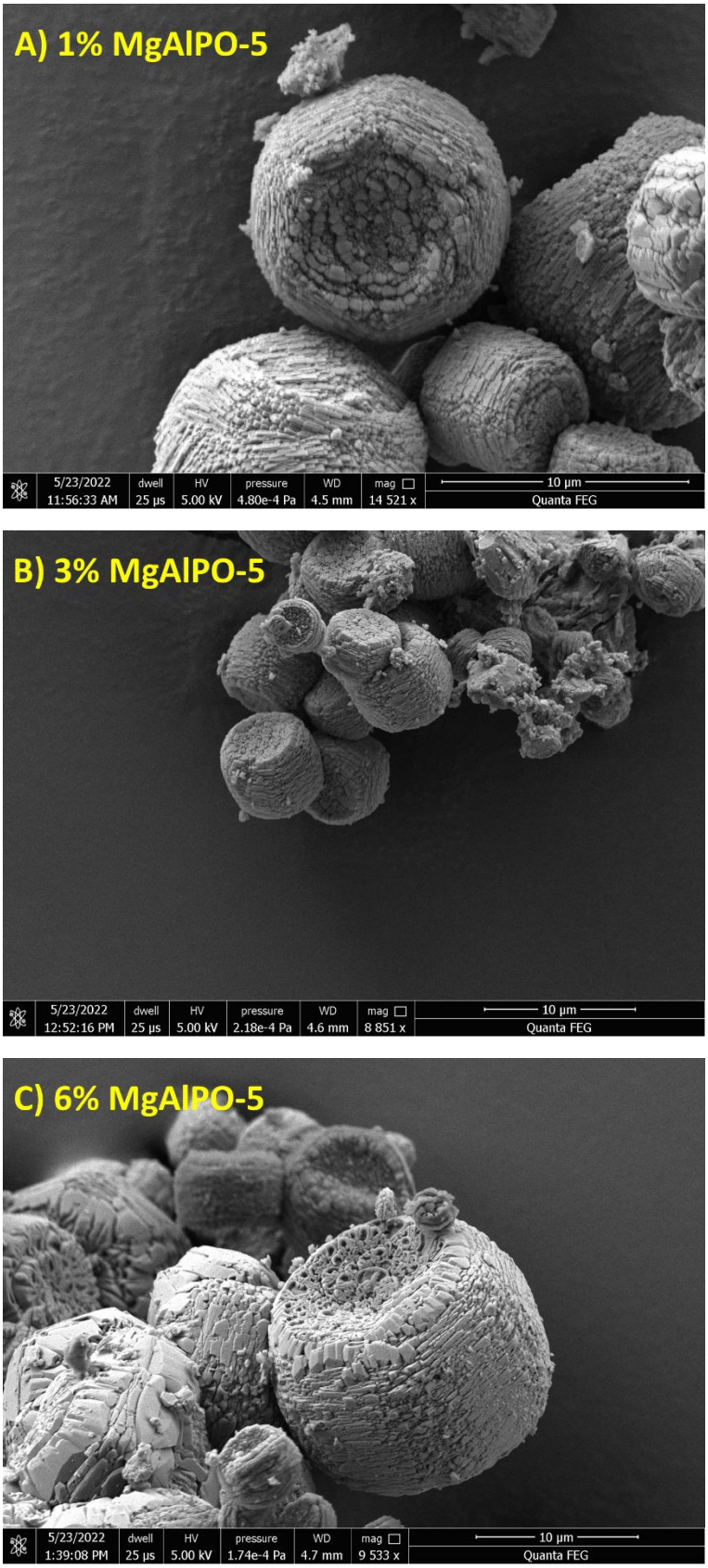

Figure S7: SEM images of MgAlPO-5 systems showing spherical/barrel like particles of similar sizes in all species, focussing on A) 1% MgAlPO-5, B) 3% MgAlPO-5 and C) 6% MgAlPO-5.

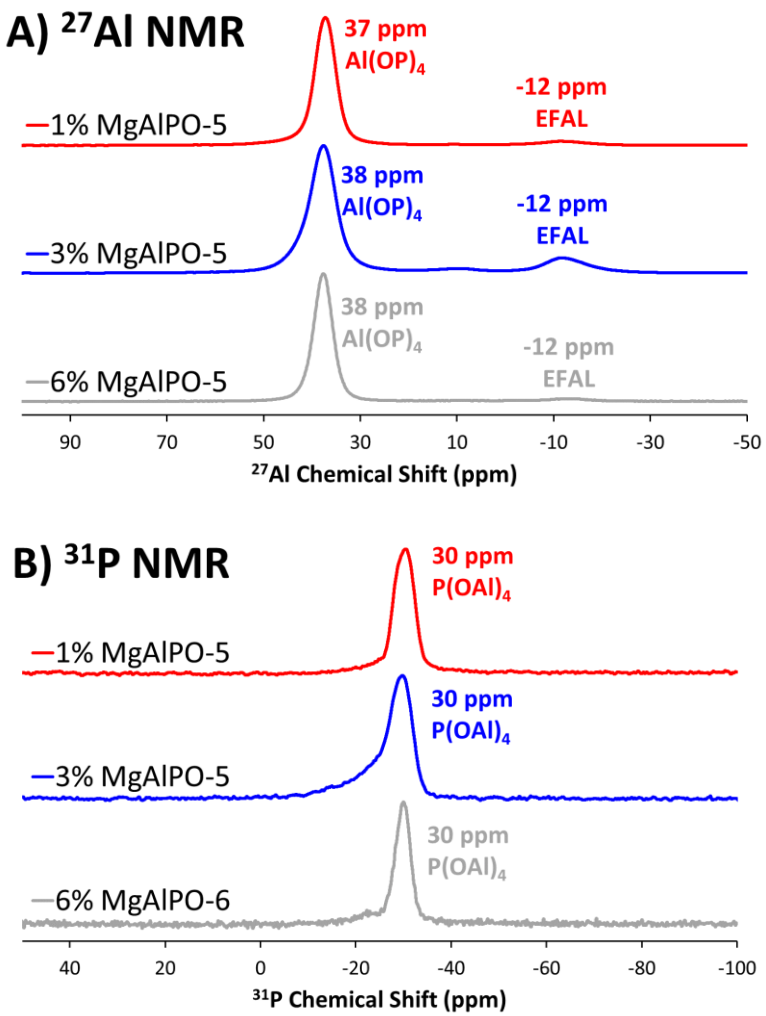

Figure S8: Solid state NMR spectra of the 3 MgAlPO-5 species focussing on A) ^{27}Al and B) ^{31}P nuclei. Both of which show predominantly tetrahedral AlO_4 and PO_4 species respectively.

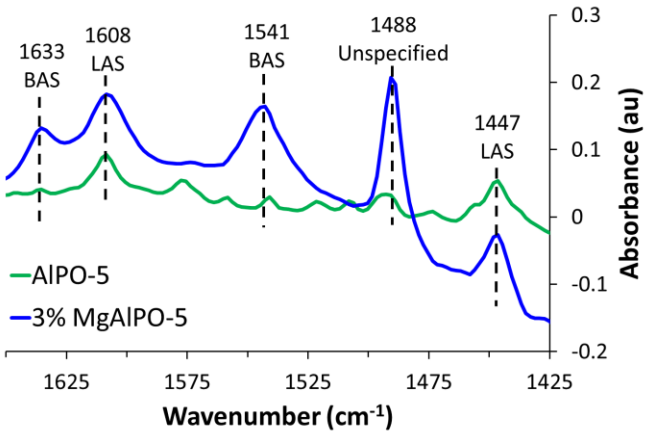

Figure S9: Pyridine-dosed DRIFTS data collected at 150 °C, comparing the acid sites present in both undoped AlPO-5 and 3% MgAlPO-5, showing the effect of incorporating Mg^{2+} into the framework. We note that in both AlPO-5 and 3% MgAlPO-5, there are strong signals at 1608 and 1447 cm^{-1} which are attributed to Lewis acid sites (LAS) present in both systems.[6-8] However on incorporating Mg^{2+} into the

framework signals increase at 1633 and 1541 cm^{-1} which are attributed purely to Bronsted acid sites (BAS). Similarly there is a growth in the signal at 1488 cm^{-1} which can be assigned to either BAS or LAS.[6-8] As such incorporating Mg^{2+} shows a clear increase in BAS, with little change in LAS, showing that introducing Mg^{2+} leads to significant formation of BAS, as expected.

Table S3: NH_3-TPD metrics for MgAlPO-5 samples.

Sample	2nd Peak Area (µmol/g)	Expected Acidity (µmol/g)[a]	Maximum Peak Temperature (°C)
1% MgAlPO-5	118	82	433
3% MgAlPO-5	234	246	417
6% MgAlPO-5	496	492	421

a) Calculated based on a molecular formula of $H_xMg_xAl_{1-x}P_1O_4$, where x = 1, 3 or 6.

Catalytic Data

Table S4: Low partial pressure flow rates for n-butane catalytic isomerisation.

Nitrogen flow (mL/min)	n-Butane flow (mL/min)	n-Butane flow (µmol/g_{cat}/sec)[a]	Total flow (mL/min)	n-Butane partial pressure (Bar)
3.15	0.76	0.863	3.91	0.194
3.25	0.68	0.777	3.93	0.174
3.31	0.61	0.690	3.92	0.155
3.41	0.53	0.604	3.94	0.135
3.47	0.46	0.518	3.93	0.116
3.53	0.38	0.431	3.91	0.097
3.63	0.30	0.345	3.93	0.077
3.69	0.23	0.259	3.92	0.058

a) Based on molar gas volume and 0.6 g of catalyst.

3% MgAlPO-5 low pressure (0.05 – 0.20 Bar)

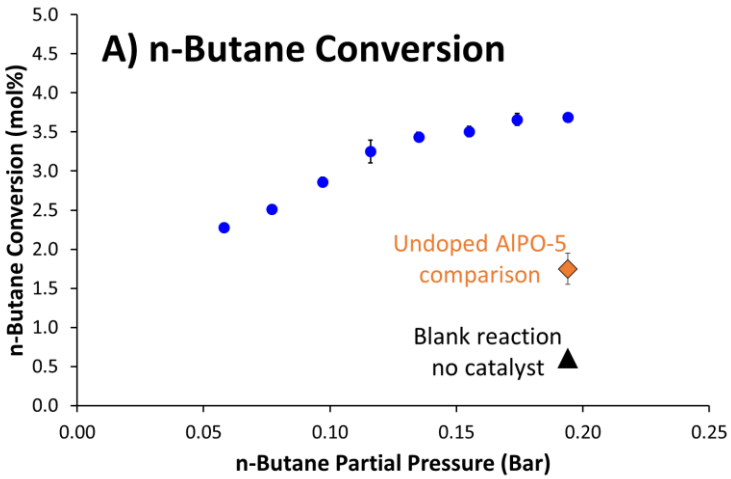

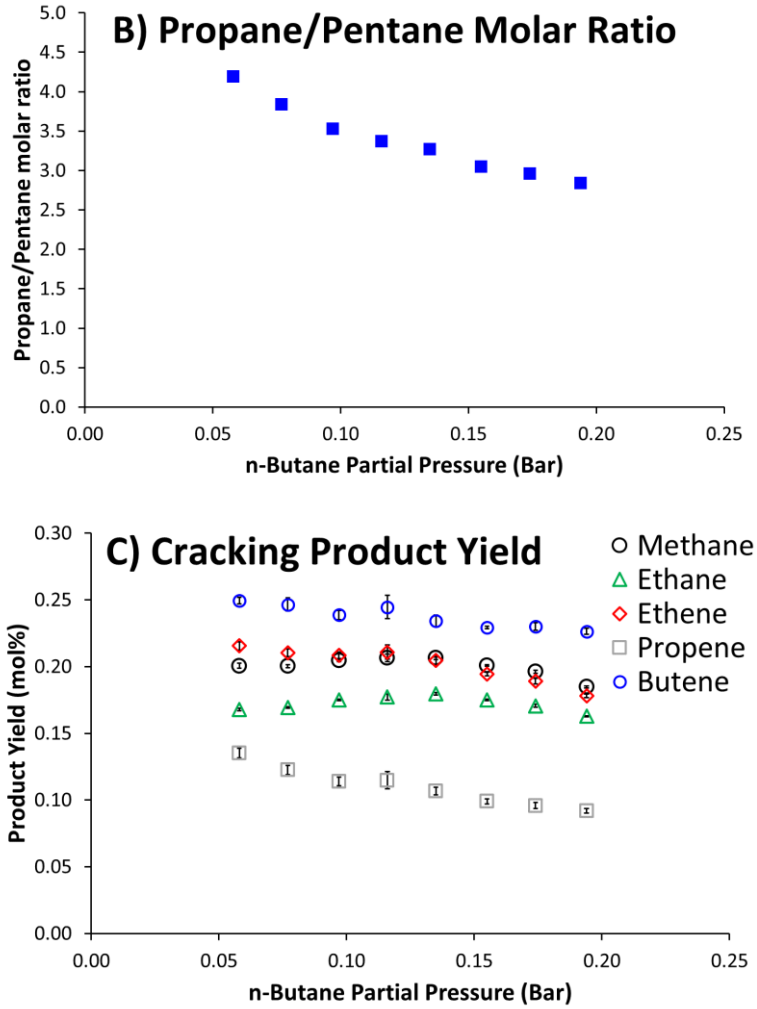

Figure S10: Catalytic data of 3% MgAlPO-5 showing the variation A) n-Butane Conversion, with undoped AlPO-5 data as a comparison, B) Propane/Pentane molar ratio, and C) Product yield of cracking products, as a function of n-butane partial pressure between 0.05 and 0.20 Bar. Conditions: 0.6 g of catalyst, 400 °C, flow rates as per Table S4.

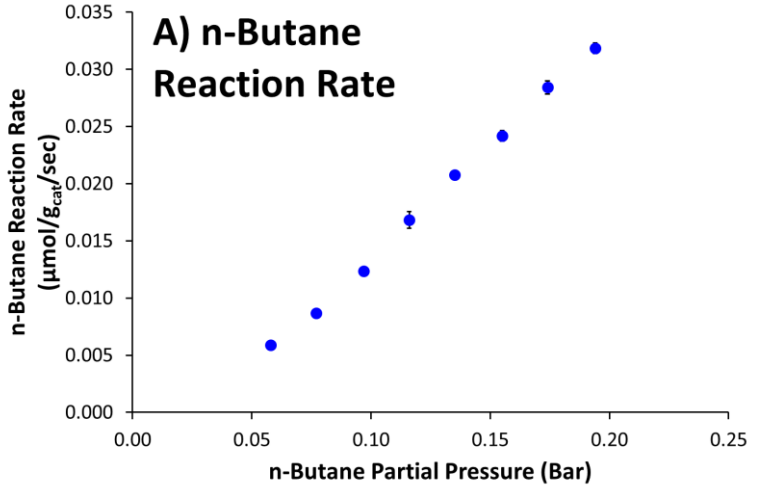

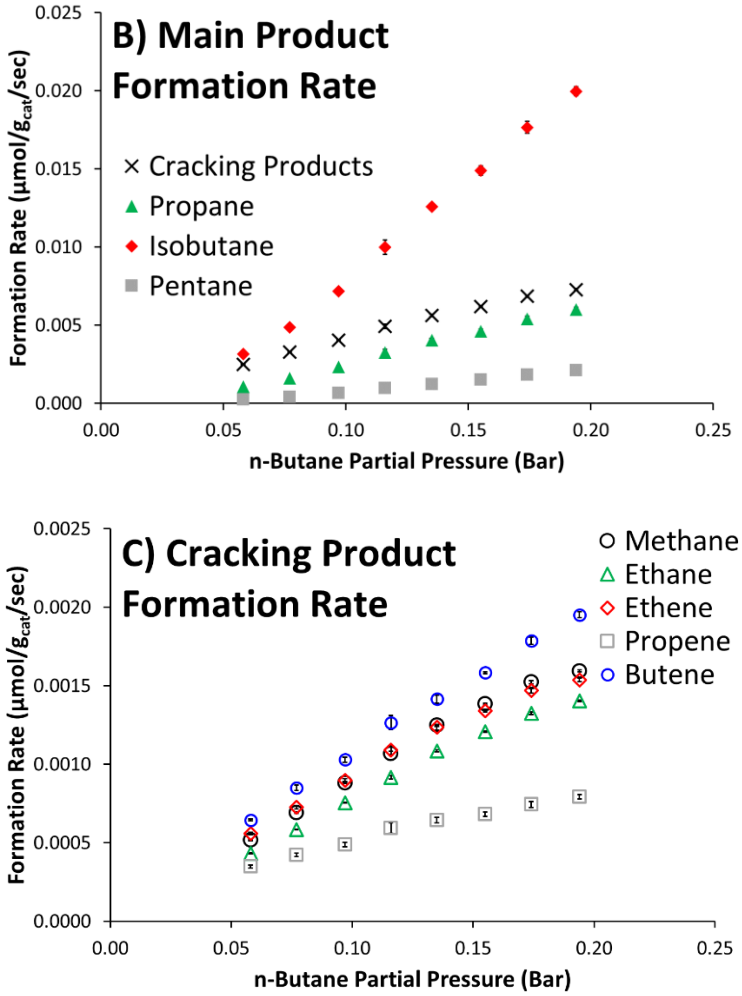

Figure S11: Catalytic data of 3% MgAlPO-5 showing the variation in A) n-Butane reaction rate, B) Primary product formation rate and C) Cracking product formation rate, as a function of n-butane partial pressure between 0.05 and 0.20 Bar. Conditions: 0.6 g of catalyst, 400 °C, flow rates as per Table S4.

3% MgAlPO-5 high pressure (0.30 – 1.00 Bar)

Table S5: High partial pressure (0.30 – 1.00) flow rates for n-butane catalytic isomerisation.

Nitrogen flow (mL/min)	n-Butane flow (mL/min)	n-Butane flow (µmol/g_{cat}/sec)[a]	Total flow (mL/min)	n-Butane partial pressure (Bar)
0.00	3.93	4.461	3.93	1.000
0.79	3.13	3.555	3.92	0.799
1.17	2.74	3.115	3.91	0.702
1.58	2.36	2.675	3.92	0.599
1.96	1.97	2.235	3.93	0.502
2.33	1.60	1.812	3.93	0.406
2.74	1.19	1.346	3.93	0.302

a) Based on molar gas volume and 0.6 g of catalyst.

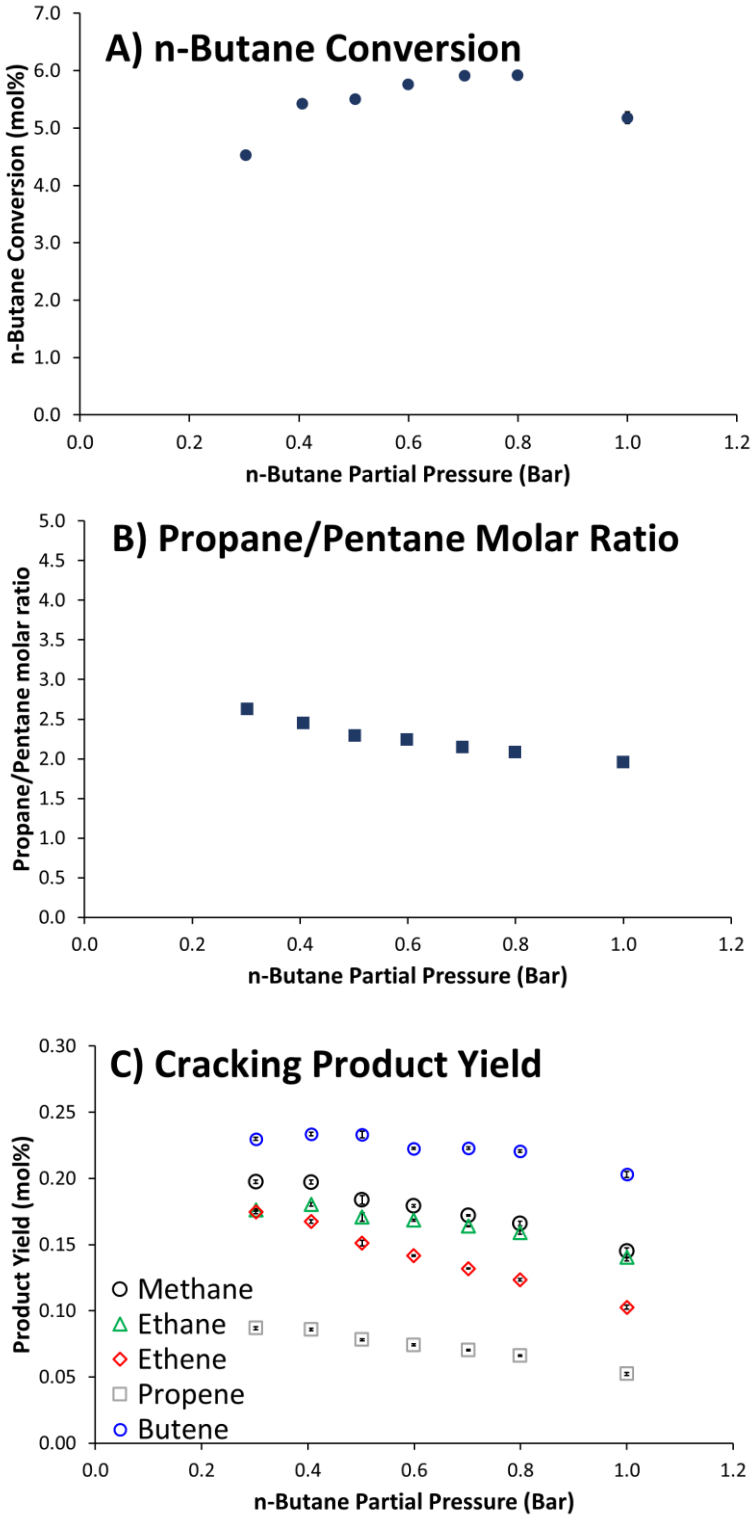

Figure S12: Catalytic data of 3% MgAlPO-5 showing the variation A) n-Butane conversion, B) Propane/Pentane molar ratio, and C) Product yield of cracking products, as a function of n-butane partial pressure between 0.30 and 1.00 Bar. Conditions: 0.6 g of catalyst, 400 °C, flow rates as per Table S5.

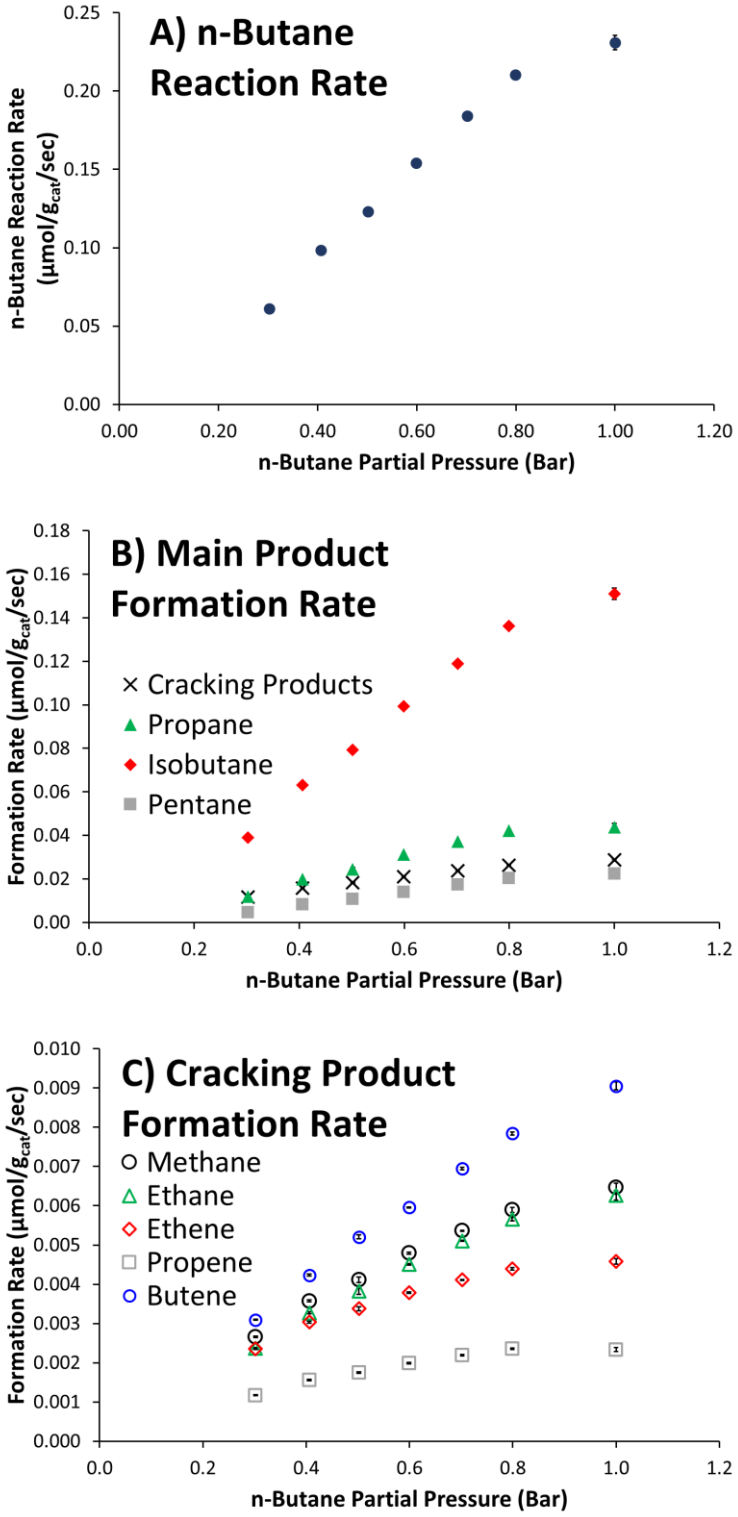

Figure S13: Catalytic data of 3% MgAlPO-5 showing the variation in A) n-Butane reaction rate, B) Primary product formation rate and C) Cracking product formation rate, as a function of n-butane partial pressure between 0.30 and 1.00 Bar. Conditions: 0.6 g of catalyst, 400 °C, flow rates as per Table S5.

Comparing high and low partial pressure activity for 3% MgAlPO-5

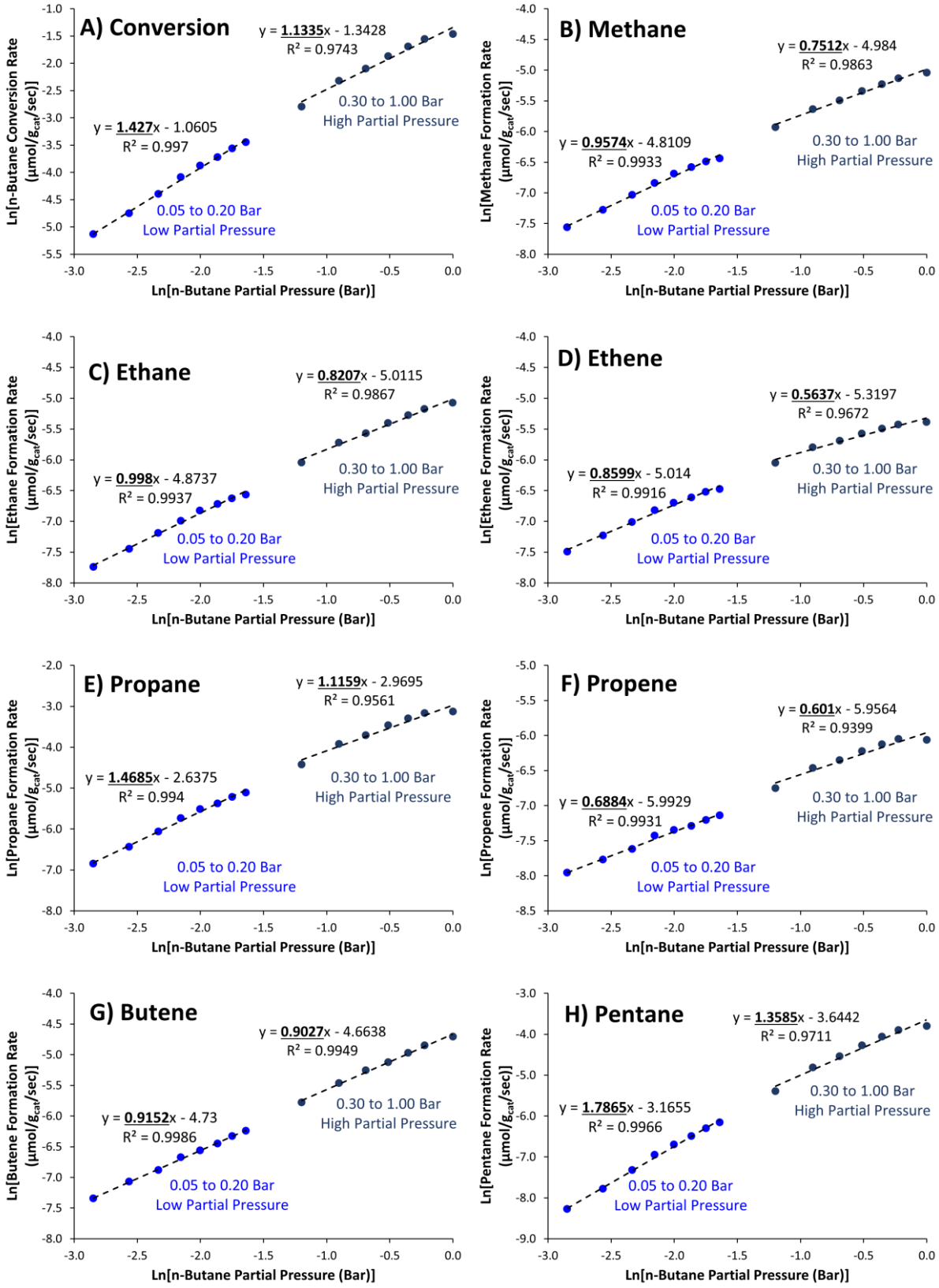

Figure S14: Deriving the reaction orders with respect to n-butane for A) n-Butane consumption, B) Methane formation, C) Ethane formation, D) Ethene formation, E) Propane formation, F) Propene Formation, G) Butene Formation and H) Pentane formation, as a function of n-butane partial pressure

between 0.05 and 0.20 Bar, and 0.30 and 1.00 Bar. Conditions: 0.6 g of catalyst, 400 °C, flow rates as per Tables S4 & S5. The values for the reaction order are summarised in Table 1 of the main text.

Low partial pressure activity for 1% & 6% MgAlPO-5

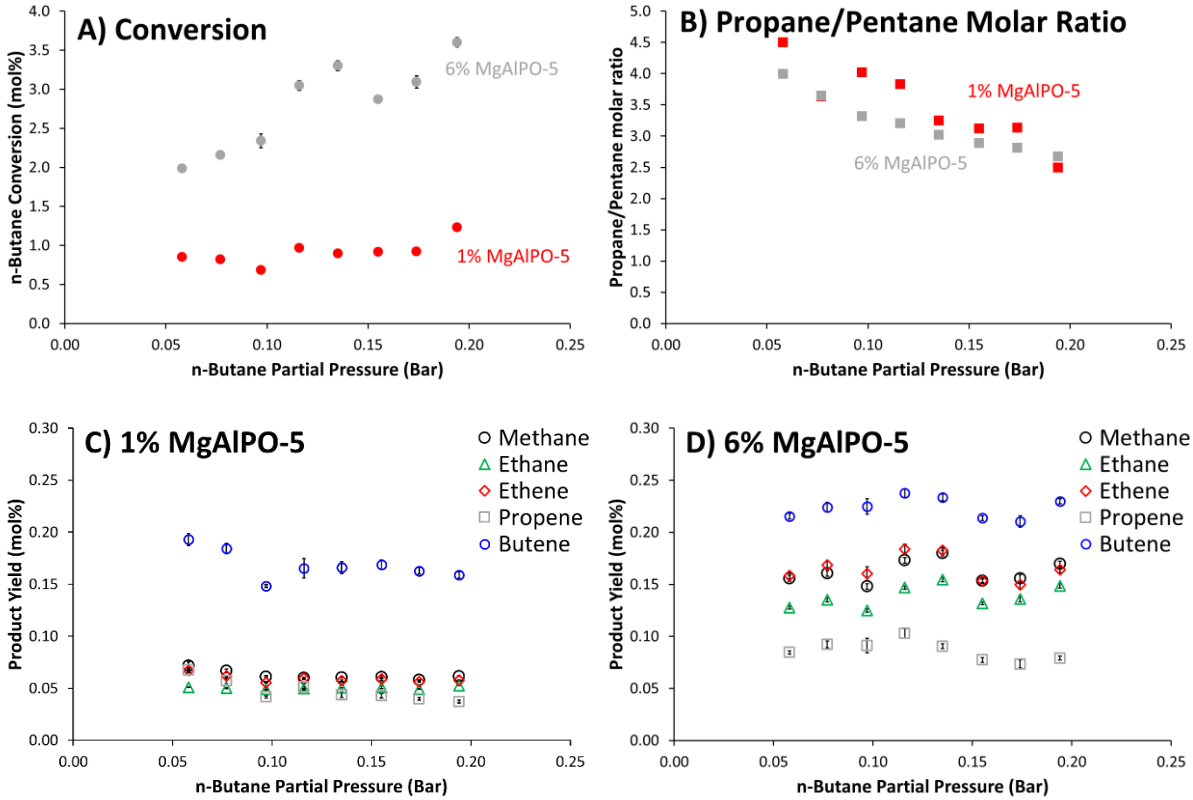

Figure S15: Catalytic data of 1% & 6% MgAlPO-5 showing the variation in: A) Conversion, B) Molar ratio of propane to pentane, C) Product yield of cracking products for 1% MgAlPO-5 and D) Product yield of cracking products for 6% MgAlPO-5, as a function of n-butane partial pressure between 0.05 and 0.20 Bar. Conditions: 0.6 g of catalyst, 400 °C, flow rates as per Table S4.

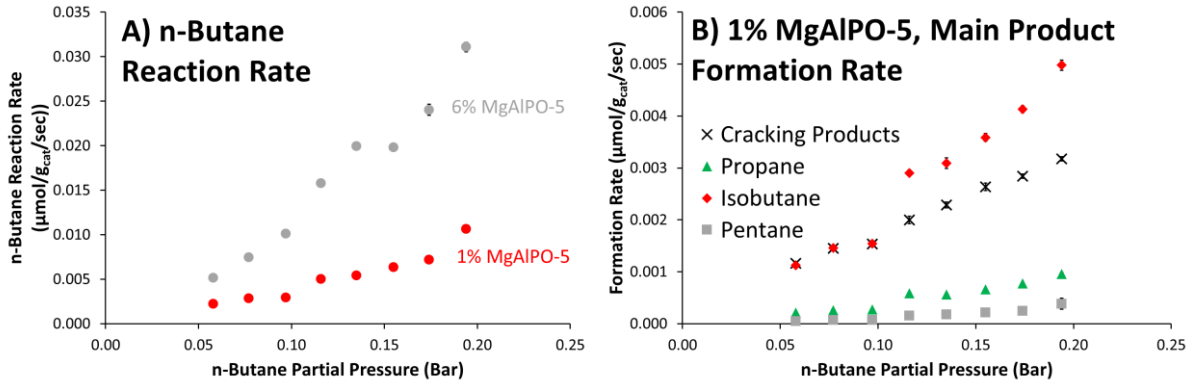

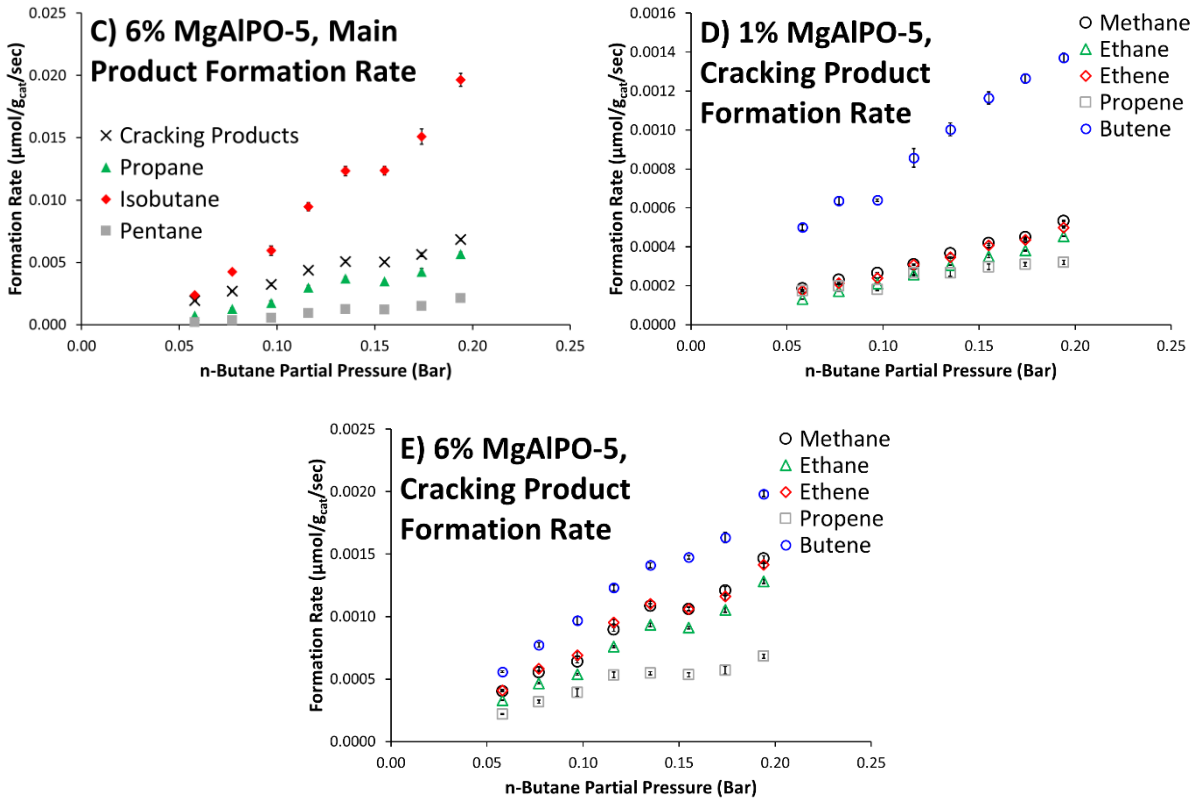

Figure S16: Catalytic data of 1% & 6% MgAlPO-5 showing the variation in: A) n-Butane reaction rate, B) Main product formation rate for 1% MgAlPO-5, C) Main product formation rate for 6% MgAlPO-5, D) Cracking product formation rate for 1% MgAlPO-5, and E) Cracking product formation rate for 6% MgAlPO-5, as a function of n-butane partial pressure between 0.05 and 0.20 Bar. Conditions: 0.6 g of catalyst, 400 °C, flow rates as per Table S4.

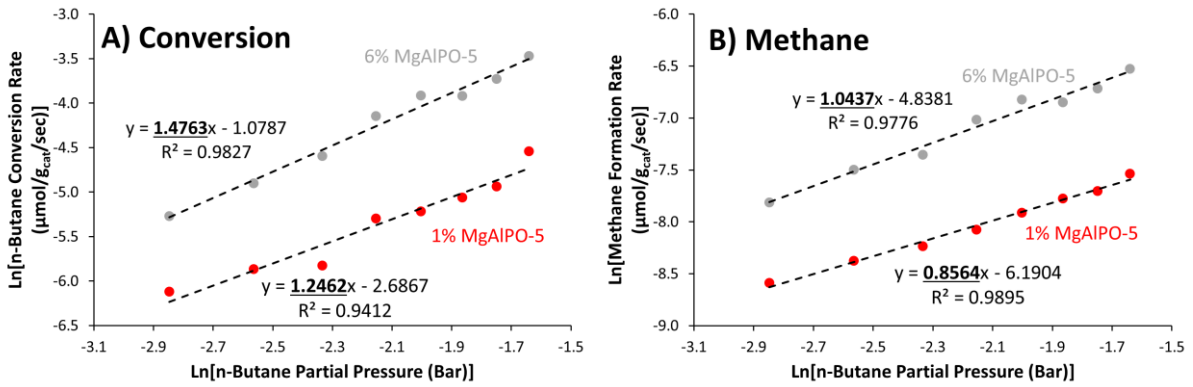

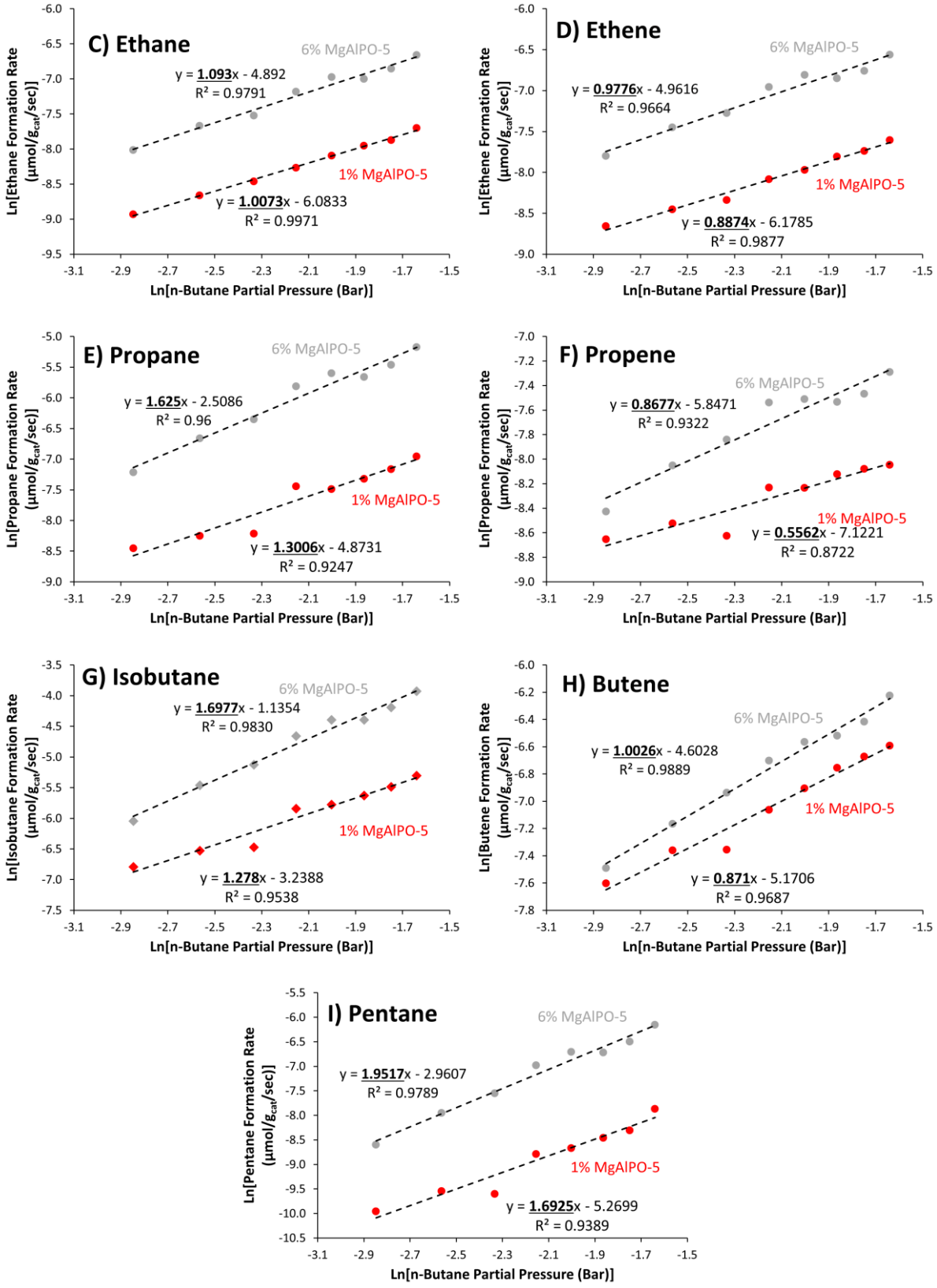

Figure S17: Deriving the reaction orders with respect to n-butane for A) n-Butane consumption, B) Methane formation, C) Ethane formation, D) Ethene formation, E) Propane formation, F) Propene Formation, G) Isobutane Formation, H) Butene formation and I) Pentene formation, as a function of n-butane partial pressure between 0.05 and 0.20 Bar for 1% & 6% MgAlPO-5. Conditions: 0.6 g of

catalyst, 400 °C, flow rates as per Tables S4. The values for the reaction order are summarised in Figure 7 of the main text.

Table S6: Calculated results of kinetic modelling fittings for the 3% MgAlPO-5 data, covering the whole n-butane partial pressure range, 0 – 1 bar, varying the equation from Wang *et al.*[9]

Parameter	$r_{bi} = \frac{AP^2}{1 + BP + CP^2}$	$r_{bi} = \frac{AP^2}{1 + BP}$	$r_{bi} = \frac{AP^2}{1 + CP^2}$
A_{Value}	3.40 x 10^{-5}	9.72 x 10^{-5}	2.69 x 10^{-5}
A_{Error}	6.54 x 10^{-6}	3.45 x 10^{-5}	1.37 x 10^{-6}
$A_{\%Error}$	19.3	35.5	5.1
B_{Value}	0.908	10.59	N/A
B_{Error}	0.833	4.29	N/A
$B_{\%Error}$	91.7	40.5	N/A
C_{Value}	2.40	N/A	2.45
C_{Error}	0.27	N/A	0.22
$C_{\%Error}$	11.1	N/A	8.9
Sum of %Errors	**122.1**	**76.0**	**14.0**

Further DFT Calculations

Potential Energy Surfaces

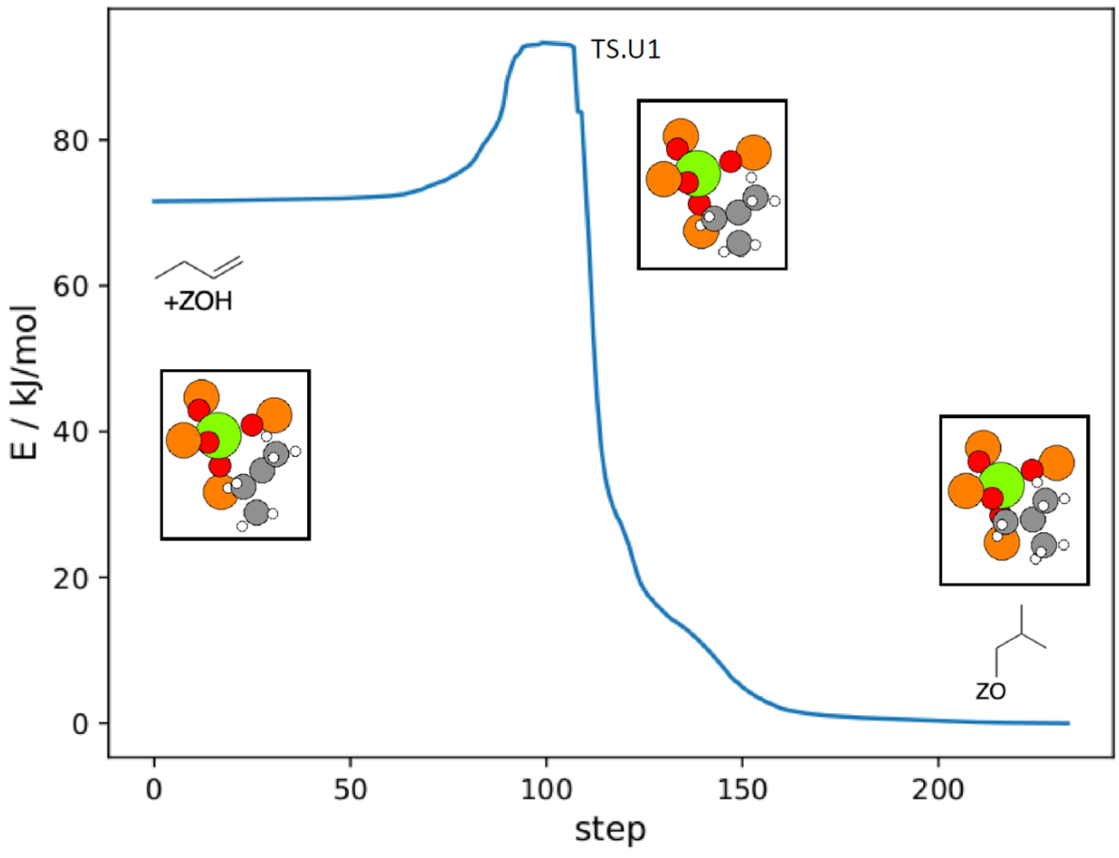

Figure S18: Calculated reaction pathway to find the energy barrier of 1-butene, forming an isobutoxide species with MgAlPO-5, *via* the TS.U1 transition state (from left to right), as detailed in Figure 6 of the main paper. Note, in these calculations, multiple steps are calculated, and not single geometries, unlike in Figure 6 of the main paper. Going from the transition state to the adsorbed butene (left-hand side), relaxations could only ever go downhill in energy to achieve a smooth relaxation profile. Thus, the left-hand side of the potential energy surface is a local minimum, unlike in Figure 6 where the system is a global minimum. To have the exact same energy as the equivalent species in Figure 6, would require a small activation barrier to be overcome, which was not permitted in the calculates for Figure S18. This is also the case for Figures S19 and S20.

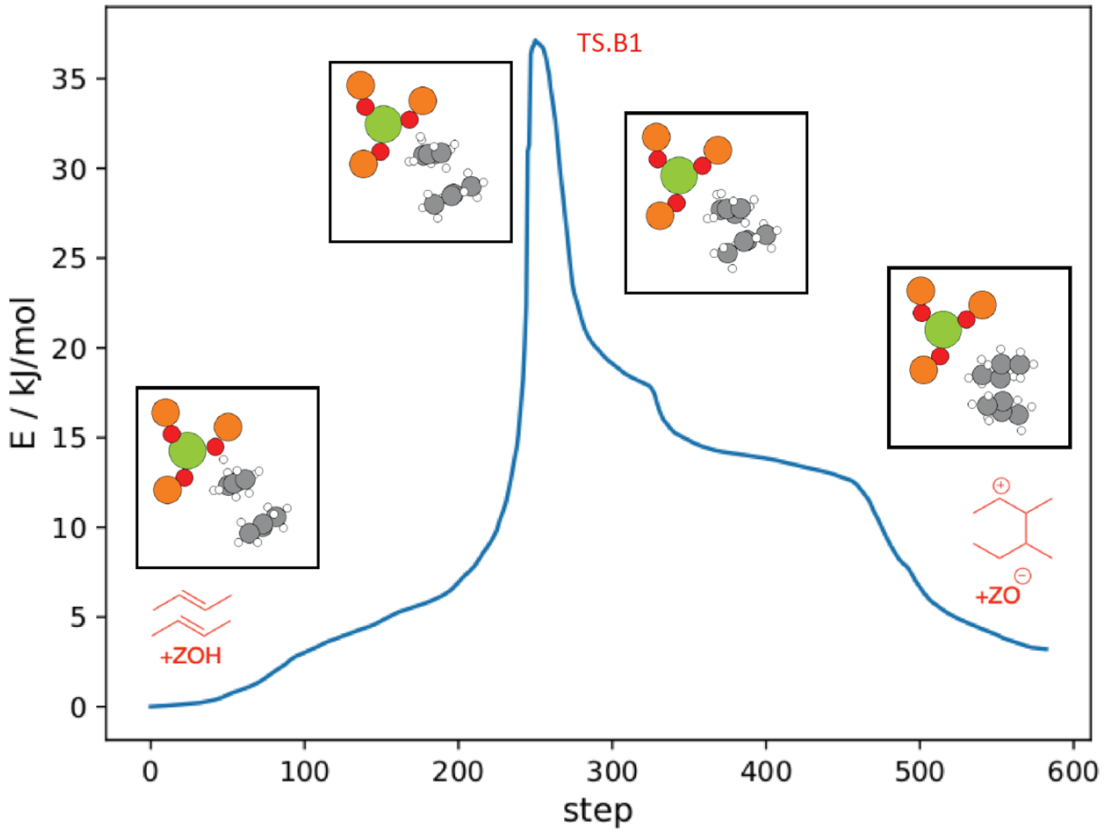

Figure S19: Calculated reaction pathway to find the energy barrier of two 2-butene species, forming an C_8 intermediate with MgAlPO-5, *via* the TS.B1 transition state (from left to right), as detailed in Figure 6 of the main paper.

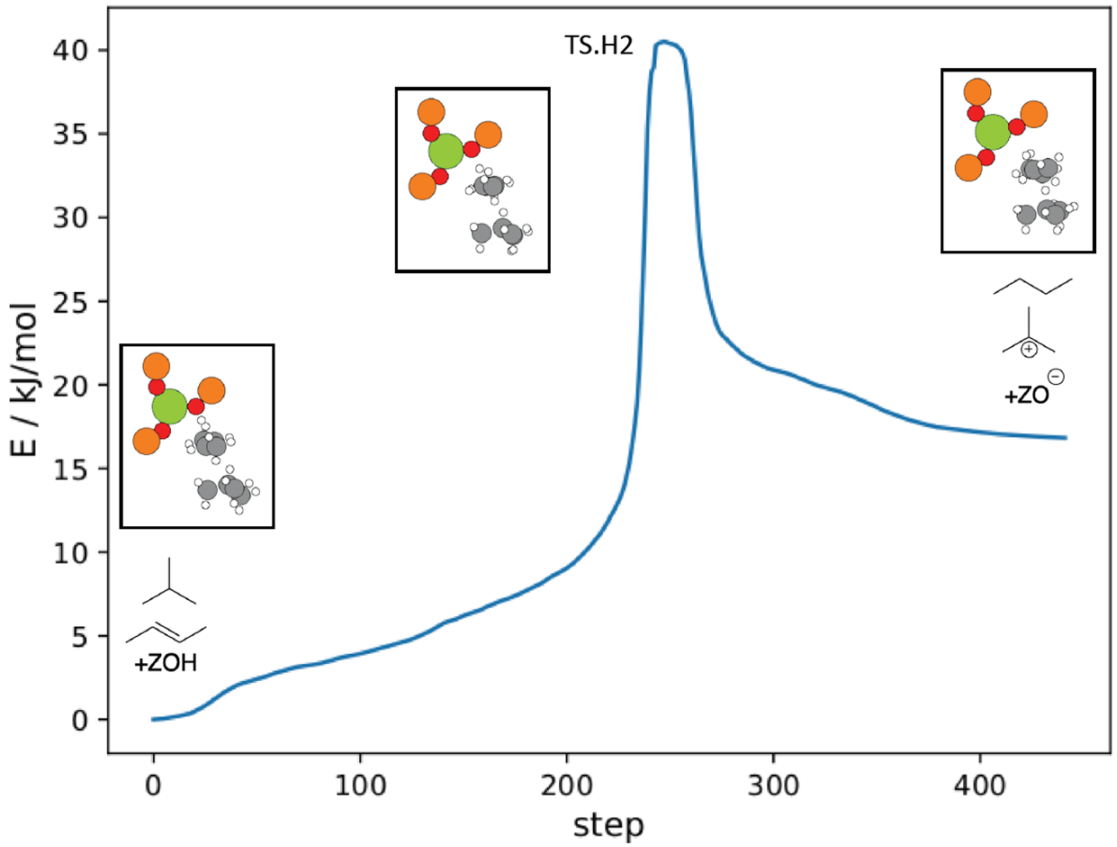

Figure S20: Calculated reaction pathway to find the energy barrier of a tertiary carbocation and n-butane, reforming the MgAlPO-5 Brönsted acid site, leading to iso-butane and 2-butene (from right to left).

Vibrational Calculations

Periodic PBE-D3 energies, Zero-point vibrational energies, cluster-model PBE-D3 energies, cluster-model M06 energies, D3 dispersion correction energies and Gibbs free energies are listed in Table S7. The harmonic frequencies of the structures are given in Table S8. Additionally, the cartesian coordinates of the structures are provided in xyz as well as POSCAR format.

Table S7: Periodic PBE-D3 energies, Zero-point vibrational energies, cluster-model PBE-D3 energies, cluster-model M06 energies, D3 dispersion correction energies and Gibbs free energies of all investigated structures, given in eV. GP stands for gas phase molecules; all other structures are the respective hydrocarbons in the H-MgAlPO-5 zeolite.

Structure	PBE-D3 (PBC)	ZPVE	PBE-D3 (CM)	M06 (CM)	D3	G
GP 2-butene	-65.407	2.847	-65.409	-4276.255	-0.071	-4276.254
GP 1-butene	-65.260	2.863	-65.263	-4276.106	-0.081	-4276.103
GP isobutane	-73.703	3.475	-73.706	-4309.731	-0.120	-4309.729
GP isobutene	-65.436	2.847	-65.437	-4276.296	-0.083	-4276.295
GP n-butane	-73.658	3.493	-73.658	-4309.669	-0.107	-4309.669
ZOH clean	-1088.529	1.289	-1439.552	-749142.600	-10.134	-748791.577
1-butene	-1154.646	4.178	-1506.243	-753419.866	-10.784	-753068.269

TS.U1	-1153.765	4.158	-1505.619	-753419.380	-10.792	-753067.526
isobutoxide	-1154.733	4.284	-1506.099	-753420.040	-10.762	-753068.675
TS.U2	-1153.819	4.116	-1505.459	-753419.176	-10.813	-753067.536
isobutyl cation	-1154.718	4.093	-1506.437	-753420.081	-10.810	-753068.362
TS.U3	-1154.710	4.059	-1506.299	-753419.926	-10.810	-753068.337
isobutene	-1154.849	4.153	-1506.170	-753419.878	-10.797	-753068.558
2-butene	-1154.865	4.164	-1506.251	-753419.957	-10.788	-753068.571
2 2-butene	-1220.939	7.037	-1572.278	-757696.646	-11.610	-757345.307
TS.B1	-1220.548	6.947	-1571.965	-757696.119	-11.602	-757344.703
3,4-dimethylhexan-2-ylium ion	-1221.045	7.160	-1572.062	-757696.420	-11.540	-757345.403
TS.B2	-1220.806	7.143	-1571.665	-757696.009	-11.504	-757345.150
2,4-dimethylhexan-3-ylium ion	-1221.094	7.153	-1572.306	-757696.751	-11.574	-757345.539
TS.B3	-1220.798	7.092	-1571.763	-757696.085	-11.586	-757345.120
2,4-dimethylhexan-2-ylium ion	-1221.417	7.121	-1572.213	-757696.454	-11.592	-757345.658
TS.B4	-1220.598	6.959	-1571.882	-757696.066	-11.637	-757344.782
isobutene + 2-butene	-1220.546	7.032	-1571.397	-757695.904	-11.638	-757345.054
isobutene + n-butane	-1229.138	7.673	-1580.375	-757729.854	-11.594	-757378.617
TS.H1	-1228.989	7.561	-1580.339	-757729.798	-11.645	-757378.447
isobutyl cation + n-butane	-1228.948	7.632	-1579.778	-757729.012	-11.691	-757378.183
TS.H2	-1228.683	7.586	-1580.038	-757729.397	-11.715	-757378.043
isobutane + 2-butene	-1228.722	7.699	-1579.560	-757729.337	-11.752	-757378.499
Pyridine	-1162.074	3.724	-1513.214	-755897.785	-10.804	-755546.645

Table S8: Vibrational frequencies of investigated structures, given in cm^{-1}.

Structure	**Frequencies**
GP 2-butene	62.7i,19.9i,5.2i,8.4,27.3,41.9,169.3,226.2,241.0,278.3,495.0,730.6,855.8,954.8,960.8,1021.2,1023.6,1065.8,1133.3,1281.3,1291.1,1355.5,1356.4,1420.6,1421.5,1431.2,1440.9,1688.8,2941.6,2942.8,2990.1,2991.3,3023.2,3024.7,3039.2,3046.4
GP 1-butene	38.8i,24.5i,14.2i,11.7,18.2,50.0,102.8,225.3,307.4,426.3,634.6,772.2,843.0,899.2,956.1,991.8,1012.0,1054.4,1161.6,1241.4,1274.9,1294.1,1352.3,1402.7,1426.3,1441.9,1450.4,1655.2,2936.7,2958.2,2983.8,3028.9,3036.2,3039.9,3054.8,3141.5
GP isobutane	42.3i,23.8i,19.4i,4.6i,34.3,35.5,215.4,248.8,261.1,357.9,358.9,418.6,790.2,895.8,896.3,922.7,953.4,954.0,1158.1,1159.4,1165.5,1306.4,1308.3,1344.6,1345.7,1372.7,1424.5,1433.2,1433.2,1450.4,1451.7,1460.4,2926.0,2944.9,2945.6,2951.2,3012.0,3012.7,3020.3,3024.5,3027.0,3027.9
GP isobutene	49.3i,25.5i,7.3i,20.1,45.5,48.1,163.1,201.7,373.1,428.5,430.2,676.7,809.3,874.0,927.9,959.7,978.6,1044.7,1058.6,1260.3,1351.7,1353.8,1388.9,1411.4,1425.0,1430.9,1446.7,1665.1,2940.5,2945.3,2990.7,2993.3,3042.7,3046.0,3058.0,3141.0
GP n-butane	7.0i,2.5i,1.5i,41.8,56.0,60.1,126.7,229.8,252.0,264.7,414.0,716.2,785.6,826.7,931.7,953.0,1003.4,1052.6,1134.4,1162.7,1242.4,1271.9,1286.5,1340.0,1355.6,1357.7,1430.5,1435.5,1444.8,1446.6,1450.3,1455.3,2932.2,2941.4,2953.8,2954.5,2954.6,2979.4,3019.7,3022.0,3029.6,3030.3
ZOH clean	199.1,239.3,244.5,260.7,275.6,291.6,298.1,343.0,358.2,377.0,395.6,459.2,537.4,594.1,621.3,623.6,713.2,719.6,728.2,737.8,746.5,750.1,775.9,799.0,862.5,1119.5,1122.3,1156.5,1252.3,3198.5
1-butene	11.7,46.8,69.1,76.1,97.5,118.9,166.7,209.5,224.3,246.6,254.3,259.9,279.2,286.2,292.6,328.9,333.8,372.6,384.9,403.7,432.6,481.9,539.9,607.6,619.9,661.9,718.9,725.2,725.9,

	730.0,735.1,739.8,749.4,781.6,783.2,803.8,850.3,891.3,938.5,962.3,1005.2,1025.1,1058.1,1115.7,1127.6,1156.8,1167.6,1243.8,1249.3,1278.6,1298.1,1357.3,1403.7,1426.5,1443.9,1452.3,1621.5,2782.0,2961.3,2967.9,3004.6,3033.3,3040.8,3045.5,3052.6,3134.1
TS.U1	134.1i,26.5,75.7,85.0,88.4,113.1,153.2,154.0,230.0,245.9,248.0,258.0,265.9,287.8,292.3,304.9,314.1,351.5,356.7,389.3,402.0,423.7,509.3,524.1,568.1,580.1,591.9,714.3,718.3,724.3,726.3,729.5,740.0,750.0,751.9,806.1,840.9,894.7,937.1,1004.3,1010.8,1084.9,1101.7,1107.3,1120.6,1141.5,1172.7,1178.0,1256.2,1269.2,1355.4,1371.6,1397.7,1408.0,1423.3,1440.7,1506.9,2935.1,2975.9,3044.8,3052.2,3063.6,3065.0,3085.7,3147.3,3177.9
isobutoxide	25.2,60.0,87.7,128.4,161.6,212.9,224.3,232.1,244.7,254.1,269.1,282.0,289.2,294.3,323.1,335.9,366.1,369.8,392.0,419.1,457.8,535.1,543.6,614.5,616.7,719.0,729.6,730.4,739.8,750.9,754.5,774.7,783.5,811.5,820.1,879.4,898.7,906.1,934.3,950.8,1115.6,1124.0,1127.0,1147.9,1160.3,1166.4,1259.7,1286.9,1326.0,1352.4,1368.6,1390.4,1427.9,1435.0,1442.1,1451.6,1459.8,2954.3,2960.8,2967.7,3005.8,3032.0,3037.1,3044.6,3064.7,3068.1
TS.U2	486.2i,40.3,69.0,83.2,92.8,131.9,191.1,205.0,230.5,245.4,252.6,260.7,280.1,283.8,296.3,306.2,329.7,366.1,382.3,386.1,423.9,428.2,518.1,549.8,581.4,591.9,596.9,717.8,721.4,725.2,732.5,734.8,740.9,742.9,757.1,761.2,825.6,931.5,951.4,993.9,1025.2,1043.3,1068.6,1085.5,1108.4,1131.1,1142.7,1167.8,1274.7,1354.8,1363.2,1368.6,1411.5,1424.1,1426.6,1451.2,1491.8,2160.4,2969.6,2982.1,3043.9,3051.1,3058.3,3073.2,3080.6,3177.1
isobutyl cation	44.2,58.7,67.9,82.8,103.1,113.8,123.6,189.0,237.3,246.9,259.0,268.9,280.6,295.7,303.9,318.7,367.9,384.9,398.7,405.5,420.4,467.9,497.0,528.8,553.0,586.2,597.8,712.2,718.3,721.3,724.4,729.1,735.2,737.4,744.9,763.1,786.2,854.0,954.2,969.0,1010.0,1052.8,1058.4,1111.9,1127.7,1168.1,1229.6,1273.4,1283.1,1308.0,1326.3,1346.3,1379.6,1382.2,1444.6,1449.7,1481.6,2155.8,2897.0,2917.2,2996.6,3004.4,3014.5,3070.4,3079.8,3105.8
TS.U3	110.5i,49.7,65.7,78.4,94.5,114.8,135.4,187.3,236.1,242.1,257.3,267.5,279.4,291.3,300.6,322.8,339.9,377.6,396.5,401.5,428.1,483.6,504.1,539.7,592.6,603.1,647.8,716.4,724.5,726.2,730.2,735.5,739.1,750.1,761.2,777.6,813.5,877.6,919.8,938.7,981.6,1029.3,1050.7,1115.9,1127.9,1151.1,1176.7,1278.1,1282.4,1308.6,1326.4,1346.5,1385.0,1399.1,1405.9,1441.7,1450.5,1585.1,2932.4,2939.3,3005.4,3014.6,3021.3,3072.9,3075.1,3116.8
isobutene	16.7,41.4,52.0,75.3,107.2,152.8,172.5,207.8,216.4,243.4,254.3,259.0,275.2,284.3,291.6,326.7,357.6,381.5,384.7,398.1,430.3,453.6,469.9,540.1,603.7,617.5,699.5,714.5,725.8,728.8,741.8,746.1,750.4,771.0,790.9,800.4,813.9,877.0,907.4,928.1,962.6,980.8,1048.9,1059.6,1124.3,1128.3,1162.3,1237.4,1272.0,1353.5,1356.4,1380.6,1409.9,1420.2,1435.0,1447.9,1625.3,2727.7,2952.2,2958.9,3007.3,3024.5,3047.0,3056.1,3059.6,3141.3
2-butene	48.0,65.9,71.6,85.4,109.7,144.6,199.5,209.5,242.7,251.3,255.1,261.1,272.5,276.8,283.0,286.5,292.2,338.0,372.2,390.1,402.3,479.8,492.7,541.2,609.5,616.2,716.6,722.3,729.1,730.5,735.4,745.3,753.4,771.7,796.5,809.2,855.3,897.6,960.8,996.6,1029.2,1040.1,1065.5,1119.0,1125.0,1138.6,1156.0,1268.2,1289.8,1303.0,1358.4,1360.6,1422.1,1424.0,1433.1,1444.5,1651.1,2627.7,2952.8,2953.6,3005.6,3009.3,3031.0,3034.9,3051.5,3056.7
2 2-butene	22.4,41.2,47.4,49.8,54.1,64.6,78.4,88.6,99.2,121.3,137.2,152.8,179.4,198.4,215.2,233.2,245.3,250.5,253.0,256.7,265.9,278.6,281.6,284.7,285.9,288.7,297.4,338.4,373.2,393.2,403.8,481.0,492.2,495.8,540.5,608.8,614.0,717.5,722.1,725.9,727.0,730.6,733.1,744.3,746.7,769.0,801.2,813.2,853.6,856.2,898.7,952.5,961.0,961.4,994.0,1020.3,1022.0,1028.4,1040.0,1066.5,1068.9,1120.3,1126.7,1134.3,1139.4,1157.3,1282.3,1283.4,1286.8,1291.9,1300.5,1352.3,1355.6,1358.3,1360.9,1417.6,1420.5,1423.8,1426.7,1431.9,1433.4,1441.4,1446.3,1649.1,1686.3,2540.0,2942.2,2953.5,2954.6,2957.6,2999.0,3003.1,3009.4,3014.0,3025.6,3031.1,3033.3,3038.5,3048.3,3052.3,3054.8,3060.8
TS.B1	220.7i,2.2,17.5,44.5,59.1,68.5,74.3,79.2,95.9,110.1,133.2,167.8,187.7,196.9,204.4,236.8,244.3,245.3,255.7,262.8,270.2,284.1,286.5,289.4,293.2,306.1,322.0,329.4,356.9,370.4,392.6,480.0,496.1,512.8,539.2,589.9,600.0,707.0,712.1,724.1,726.0,735.0,738.1,742.

	6,744.9,748.4,777.7,802.9,851.5,856.8,891.8,933.9,955.8,964.2,980.0,1017.7,1021.1,1037.2,1065.2,1073.3,1120.4,1127.5,1140.1,1142.9,1144.0,1158.2,1201.6,1250.7,1282.6,1290.7,1293.4,1330.2,1354.7,1358.6,1363.1,1380.1,1399.3,1418.7,1421.0,1429.5,1431.4,1435.6,1442.4,1448.8,1598.6,1662.8,2932.5,2940.1,2951.6,2971.9,2992.8,3004.5,3005.7,3022.8,3026.8,3033.3,3039.5,3049.1,3054.9,3058.1,3059.1,3083.7
34-dimethylhexan-2-ylium ion	8.9,27.7,39.7,60.5,68.2,86.5,95.4,124.9,160.5,216.2,222.6,231.5,241.1,248.1,256.4,261.9,265.7,269.5,274.8,284.1,294.0,298.9,303.7,305.8,328.2,357.6,380.1,387.3,397.5,412.7,450.7,495.0,525.6,538.6,578.2,582.2,587.1,708.3,719.4,720.5,722.4,734.4,741.0,744.6,752.7,766.8,771.2,809.0,867.4,948.1,969.2,980.0,986.0,1003.0,1011.8,1047.3,1061.7,1109.6,1112.2,1116.2,1121.3,1139.8,1144.9,1174.5,1184.9,1227.3,1247.8,1276.8,1285.8,1294.8,1305.8,1312.6,1360.9,1367.6,1371.8,1379.7,1421.0,1425.9,1430.9,1434.7,1442.7,1448.1,1452.8,1456.1,1511.5,2877.4,2914.6,2955.1,2964.3,2975.3,2981.2,2999.0,3023.0,3030.9,3033.8,3047.0,3051.9,3059.8,3060.9,3067.4,3073.1,3094.6
TS.B2	122.4i,22.3,25.4,55.6,61.7,73.0,84.7,105.5,129.0,169.1,195.5,204.2,221.6,223.4,234.9,248.4,260.7,264.5,270.7,279.8,283.4,291.4,302.4,319.1,321.1,354.2,375.6,376.4,386.0,441.0,460.9,483.3,521.9,567.1,568.7,581.8,585.1,703.6,711.8,716.9,718.7,727.0,732.7,738.9,744.5,747.7,807.8,819.2,871.8,906.3,934.1,957.9,989.2,1012.3,1022.4,1054.7,1087.5,1092.6,1107.6,1120.5,1135.6,1138.8,1151.6,1169.9,1190.3,1221.3,1243.3,1263.5,1277.4,1283.3,1308.2,1347.8,1360.7,1367.2,1369.4,1387.7,1398.6,1421.1,1430.6,1438.9,1442.0,1448.3,1449.3,1451.2,1530.0,2907.7,2950.7,2959.7,2962.2,2965.8,2978.0,3014.5,3017.0,3030.2,3034.4,3041.8,3049.6,3054.6,3067.3,3067.7,3086.9,3133.4
2,4-dimethylhexan-3-ylium ion	37.2,49.3,56.0,65.7,69.2,80.5,96.7,132.7,147.2,208.0,214.8,223.9,229.5,235.8,243.3,255.9,260.7,264.5,270.3,284.0,284.9,298.4,320.7,327.9,341.1,355.1,375.1,388.1,397.8,440.4,444.5,523.7,534.5,571.0,583.2,588.6,593.5,712.0,720.4,722.2,726.7,731.1,737.4,745.0,752.9,776.9,811.1,862.7,909.6,916.8,942.9,958.9,971.2,989.5,1022.5,1039.4,1076.8,1096.3,1108.0,1111.3,1132.7,1145.5,1158.4,1167.9,1177.5,1215.5,1246.6,1249.9,1287.5,1299.6,1341.6,1351.8,1360.9,1367.0,1370.4,1381.7,1392.4,1426.6,1430.5,1437.9,1440.9,1445.6,1452.6,1454.9,1471.0,2504.1,2961.6,2962.2,2967.5,2970.4,2978.0,3027.8,3028.6,3032.2,3041.6,3053.8,3056.0,3057.5,3063.6,3065.7,3067.9,3101.7
TS.B3	186.9i,29.3,40.4,55.8,63.7,66.9,83.0,101.1,126.8,144.2,165.4,192.5,204.1,222.7,226.1,244.5,253.5,259.8,263.5,266.8,279.9,289.9,301.5,324.0,352.2,364.6,374.5,388.7,391.4,426.8,446.5,494.4,522.6,570.7,579.2,583.2,648.7,710.8,716.0,720.9,722.6,728.3,735.2,738.6,741.8,752.9,761.0,827.5,867.3,918.3,954.1,956.7,961.6,997.9,1018.5,1023.1,1043.3,1048.4,1082.0,1119.8,1123.3,1124.9,1139.1,1149.4,1177.6,1193.3,1229.9,1264.3,1275.8,1302.4,1324.4,1356.6,1360.7,1365.8,1377.9,1398.6,1420.1,1421.7,1427.3,1431.8,1435.3,1442.8,1448.3,1452.5,1492.9,2425.5,2924.1,2964.4,2970.4,2986.1,2988.0,3000.3,3010.4,3018.7,3027.2,3049.7,3059.4,3063.8,3064.7,3068.9,3069.0,3080.8
2,4-dimethylhexan-2-ylium ion	17.3,26.4,46.7,60.6,66.7,78.6,99.6,107.0,138.7,198.1,200.6,217.1,224.1,245.3,251.3,260.6,261.7,267.0,284.8,285.2,289.2,301.1,309.6,315.9,360.5,379.0,383.8,389.3,412.7,425.4,472.6,500.6,519.7,563.2,576.6,584.9,711.1,714.0,716.4,720.6,724.9,732.7,738.0,743.9,747.3,760.5,791.6,822.4,841.9,871.1,948.8,952.0,960.8,980.8,999.0,1028.8,1065.0,1074.1,1103.3,1117.7,1122.4,1150.0,1158.3,1186.2,1212.9,1235.4,1254.8,1273.2,1280.7,1299.8,1314.3,1329.1,1336.7,1360.0,1369.0,1371.0,1376.9,1401.8,1410.3,1428.8,1444.4,1445.8,1447.8,1451.9,1454.0,2875.8,2880.6,2907.4,2927.1,2938.6,2946.9,2958.8,2970.8,2980.5,3005.9,3008.7,3025.9,3047.9,3050.9,3061.0,3079.4,3103.8
TS.B4	112.4i,15.7,32.4,39.1,54.0,61.4,73.1,82.1,96.1,113.9,131.6,150.9,171.8,187.4,216.8,232.3,239.5,247.2,256.2,262.7,276.2,286.7,288.1,304.7,309.1,323.4,359.5,380.3,394.2,407.2,434.6,444.7,474.9,510.4,551.4,585.0,599.6,697.9,711.5,712.2,722.2,724.3,738.0,743.5,745.5,755.2,761.3,811.1,832.8,844.6,874.8,926.1,927.4,955.6,962.7,980.9,985.4,1027.6,1042.6,1056.5,1063.5,1106.5,1135.5,1137.4,1152.9,1166.9,1211.9,1245.5,1269.0,1283.2,1322.6,1354.3,1356.4,1358.8,1384.9,1390.0,1399.7,1408.8,1421.8,1425.9,1432.5,1443.5,1445.9,1461.7,1622.2,1661.5,2946.8,2952.3,2957.3,2980.7,3005.8,3006.1,3009.4,3016.6,3048.0,3050.7,3055.5,3056.9,3065.9,3068.2,3091.5,3141.3
isobutene + 2-butene	16.5,32.6,35.3,48.3,51.6,60.1,67.4,78.2,85.0,93.9,107.4,132.7,170.7,180.3,198.0,198.7,228.1,240.4,250.0,258.8,267.0,277.0,278.4,292.2,300.2,339.0,355.0,372.1,375.3,397.0,428.9,434.8,467.2,492.5,537.6,550.5,590.2,623.7,678.0,709.8,718.1,723.0,726.2,734.4,745.3,751.1,778.4,802.7,815.2,854.3,873.7,878.2,933.1,952.6,958.4,963.3,980.5,1016.

isobutene + n-butane	0,1020.9,1048.5,1059.6,1066.5,1124.4,1128.8,1134.2,1160.4,1238.8,1264.1,1279.4,1295.8,1351.4,1352.7,1355.4,1358.0,1392.5,1409.7,1420.1,1420.8,1425.9,1428.3,1433.5,1441.8,1447.2,1669.7,1686.3,2941.0,2944.5,2945.8,2946.2,2992.8,2994.3,3003.2,3003.6,3025.9,3042.5,3045.7,3051.0,3056.4,3061.9,3065.9,3151.4,3248.3 3.1,45.3,50.0,61.5,63.3,67.7,79.4,90.8,92.6,106.0,110.9,145.0,156.8,183.0,211.0,223.2,229.5,239.4,251.1,253.4,258.0,270.9,285.5,288.1,327.8,329.0,358.8,382.1,389.7,397.1,426.3,432.0,459.6,471.9,541.1,602.9,617.6,706.1,712.7,726.3,727.7,729.8,736.9,746.3,748.9,763.5,771.1,782.1,805.5,815.0,817.6,880.8,913.1,927.6,936.4,954.3,964.0,964.4,980.3,1049.3,1060.8,1072.4,1115.5,1125.8,1126.5,1149.0,1161.2,1241.3,1243.8,1273.6,1274.6,1322.1,1324.1,1354.7,1356.8,1357.8,1358.3,1378.0,1410.6,1414.9,1429.9,1431.5,1434.3,1441.2,1445.6,1449.3,1451.4,1454.7,1623.3,2669.1,2928.6,2944.6,2953.4,2957.6,2960.4,2962.7,2988.4,2996.2,3011.7,3021.7,3022.7,3028.1,3031.5,3032.1,3044.1,3062.9,3070.0,3141.7
TS.H1	294.4i,24.8,44.8,51.9,59.6,62.8,66.8,76.3,87.1,97.7,115.6,139.6,152.7,161.0,181.1,227.2,231.9,243.9,255.6,256.9,262.6,281.5,289.4,293.9,318.6,322.3,326.1,363.4,393.5,401.4,422.2,432.0,483.6,505.0,542.9,586.3,597.0,659.6,708.8,716.3,720.4,726.8,727.5,729.3,739.5,755.1,756.1,771.4,771.5,814.2,826.5,839.8,886.3,937.4,939.2,951.0,961.1,983.9,1032.6,1041.6,1071.1,1101.3,1113.6,1118.3,1136.1,1149.3,1171.9,1189.8,1246.8,1271.3,1283.7,1302.3,1320.7,1328.0,1331.0,1344.4,1357.3,1358.4,1370.8,1394.1,1404.2,1430.4,1433.8,1439.8,1442.2,1449.6,1449.9,1453.6,1455.8,1572.6,2925.0,2944.1,2948.3,2953.4,2953.8,2960.4,2986.0,2986.7,3009.1,3018.1,3019.8,3021.3,3026.7,3032.4,3049.0,3077.8,3081.1,3122.9
isobutyl cation + n-butane	20.9,43.7,45.2,64.3,71.5,75.7,84.4,120.8,141.7,158.6,187.7,193.9,222.7,234.2,237.3,242.0,247.2,253.0,256.1,266.3,272.6,281.9,285.9,289.2,299.3,313.9,332.9,365.5,386.7,390.0,396.4,397.4,467.2,525.4,533.8,574.2,582.3,590.4,709.1,712.4,713.9,715.5,721.4,726.5,736.7,737.8,738.7,747.9,780.3,814.9,858.9,880.5,922.5,945.0,955.1,974.7,996.7,999.7,1001.2,1085.3,1106.6,1122.5,1125.8,1135.5,1140.8,1156.0,1190.9,1193.4,1244.0,1248.6,1254.1,1313.8,1324.2,1338.2,1339.3,1343.8,1363.3,1375.8,1384.0,1390.3,1411.0,1415.2,1420.0,1425.0,1428.8,1435.4,1444.9,1456.3,1463.8,1969.2,2927.4,2945.7,2950.1,2955.4,2966.1,2975.2,2982.1,3007.9,3022.9,3025.0,3031.2,3034.7,3046.3,3066.4,3070.3,3071.7,3074.8,3077.8
TS.H2	122.3i,24.3,44.9,55.0,60.7,65.5,68.5,94.2,105.1,129.8,131.3,158.0,186.7,220.3,230.4,245.9,249.5,255.4,258.8,260.5,274.3,280.4,282.5,284.3,304.5,323.2,335.6,358.2,366.7,368.5,380.7,395.9,438.4,475.9,516.5,543.0,592.8,597.5,675.4,712.7,722.8,727.4,735.6,735.8,741.2,748.2,770.5,788.3,829.2,854.2,886.9,889.3,920.1,927.8,954.7,962.8,970.7,994.7,1033.5,1062.0,1120.4,1128.8,1137.1,1146.8,1155.6,1159.5,1161.3,1165.4,1234.4,1246.1,1260.5,1262.7,1287.9,1326.2,1345.8,1345.9,1365.4,1373.6,1396.7,1413.9,1423.9,1426.1,1428.7,1433.3,1444.1,1450.6,1452.7,1458.2,1498.1,1773.8,2658.4,2937.8,2953.6,2958.4,2971.6,2979.8,3004.5,3010.0,3018.2,3024.9,3040.6,3042.3,3044.9,3045.5,3050.5,3053.0,3070.8,3075.7
isobutane + 2-butene	30.5,34.7,50.9,60.5,62.8,66.8,80.2,93.1,104.0,114.5,130.4,169.4,196.1,210.6,232.6,242.4,246.0,255.2,265.8,270.5,273.4,274.0,285.6,291.0,295.3,303.8,349.6,360.1,360.9,363.3,373.0,405.1,420.7,466.1,494.8,538.4,541.2,586.3,632.2,711.8,719.3,723.2,735.0,738.8,743.3,748.1,780.3,792.7,799.5,857.1,878.3,894.7,899.7,927.5,955.9,957.0,963.5,966.1,1020.2,1023.7,1065.8,1126.6,1132.8,1135.2,1162.2,1163.0,1166.3,1170.2,1238.7,1282.8,1298.9,1302.7,1313.3,1343.6,1344.6,1351.1,1357.1,1371.4,1417.3,1423.8,1428.9,1433.6,1435.5,1437.5,1450.8,1453.8,1455.5,1460.8,1685.1,2948.2,2952.2,2956.0,2958.6,2961.0,2974.8,3006.0,3015.7,3021.4,3024.3,3030.9,3033.9,3035.9,3037.6,3046.5,3048.8,3057.9,3061.8,3239.5
Pyridine	31.5,48.0,64.7,75.8,90.7,99.3,233.8,251.6,258.4,266.2,285.4,287.4,302.3,316.4,356.6,391.2,397.2,397.8,418.5,516.6,558.6,578.7,593.5,605.8,632.5,688.6,711.1,720.7,724.5,730.3,733.5,738.2,749.3,751.3,761.8,884.2,944.0,993.5,998.7,1019.1,1022.5,1059.7,1061.8,1064.1,1076.7,1111.4,1139.2,1162.8,1176.8,1195.9,1295.5,1342.2,1397.9,1473.4,1545.2,1621.3,1633.6,2849.4,3105.9,3121.0,3123.7,3131.6,3150.7

References

1. G. Kresse and J. Furthmüller, *Comput. Mater. Sci.*, 1996, **6**, 15-50.
2. G. Kresse and J. Furthmüller, *Phys. Rev. B*, 1996, **54**, 11169-11186.
3. G. Kresse and J. Hafner, *Phys. Rev. B*, 1993, **47**, 558.
4. G. Kresse and J. Hafner, *Phys. Rev. B*, 1994, **49**, 14251.
5. G. Kresse and D. Joubert, *Physical Review B*, 1999, **59**, 1758-1775.
6. D. Padovan, A. Al-Nayili and C. Hammond, *Green Chemistry*, 2017, **19**, 2846-2854.
7. R. K. Parsapur and P. Selvam, *Sci Rep*, 2018, **8**, 16291.
8. D. S. A. Silva, W. N. Castelblanco, D. H. Piva, V. de Macedo, K. T. G. Carvalho and E. A. Urquieta-González, *Molecular Catalysis*, 2020, **492**.
9. P. Wang, W. Zhang, H. Zhu, P. Yuan, C. Yang, C. Li and X. Bao, *Applied Catalysis A: General*, 2019, **584**.